Homo-and heterodinuclear complexes of the tris(catecholamide) derivative of a tetraazamacrocycle with Fe^{3+}, Cu^{2+} and Zn^{2+} metal ions†

Krassimira P. Guerra[a] and Rita Delgado*[a,b]

Received 22nd August 2007, Accepted 26th October 2007
First published as an Advance Article on the web 12th November 2007
DOI: 10.1039/b712916e

The new ditopic catecholamide 3,7,11-tris-{*N*-[3,4-(dihydroxybenzoyl)-aminopropyl]} derivative of a 14-membered tetraazamacrocycle containing pyridine (H_6L^1) has been synthesized. The protonation constants of $(L^1)^{6-}$ and the stability constants of its mono-, homo- and hetero-dinuclear complexes with Fe^{3+}, Cu^{2+} and Zn^{2+} metal ions were determined at 298.2 K and ionic strength 0.10 mol dm^{-3} in KNO_3. The large overall basicity of the ligand was ascribed to the very high protonation constants of the catecholate groups, and its acid–base behaviour was correlated with the presence of tertiary nitrogen atoms and secondary amide functions. The UV-vis spectrum of the red solution of $[FeL^1]^{3-}$ complex exhibits the LMCT band of catecholate to iron(III), and its EPR spectrum revealed a typical isotropic signal of a rhombic distorted ferric centre in a high-spin state and $E/D \approx 0.31$, both characteristic of a tris-catecholate octahedral environment. The ligand forms with copper(II) and zinc(II) ions mono- and dinuclear protonated complexes and their stability constants were determined, except for the $[ML^1]^{4-}$ complexes as the last proton is released at very high pH. Electronic spectroscopic studies of the copper complexes revealed the involvement of catecholate groups in the coordination to the metal centre in the mono- and dinuclear copper(II) complexes. This information together with the determined stability constants indicated that the copper(II) ion can be involved in both types of coordination site of the ligand with comparable binding affinity. The EPR spectrum of $[Cu_2L^1]^{2-}$ showed a well resolved seven-line hyperfine pattern of copper(II) dinuclear species typical of a paramagnetic triplet spin state with weak coupling between the two metal centres. Thermodynamically stable heterodinuclear complexes, $[CuFeH_hL^1]^{h-1}$ ($h = 0$–3) and $[CuZnH_hL^1]^{h-2}$ ($h = 0$–4), were formed as expected from a ditopic ligand having two dissimilar coordination sites. At physiological pH, the $[CuFeL^1]^-$ complex is formed at ≈100%. The formation of the $[CuFeH_hL^1]^{h-1}$ complexes in solution was supported by electronic spectroscopic measurements. The data indicated the specific coordination of each metal centre at the dissimilar sites of the ligand, the iron(III) bound to the oxygen donors of the catecholate arms and the copper(II) coordinated to the amine donors of the macrocyclic ring. The two metal centres are weakly coupled, due to the fairly large distance between them.

Introduction

Over the last twenty years a continuous interest in the search for synthetic ditopic ligands has been carried out. These ligands should provide donor atoms, coordination number and geometric dissimilarity in the two different coordination environments, and they should be capable of binding two different metal ions.[1] The recognition of homo- and heterodinuclear cores at the active sites of metalloenzymes, responsible for specific biological functions,[2] has enhanced attention to these ligands able to be used as models of such enzymes.[3–6] The coordination versatility of ditopic ligands extends their applications to catalysis, redox processes, mixed-valence chemistry or DNA interaction.[3–7] The ditopic ligands still have applications in the removal of toxic metals or radioactive isotopes.[8]

Ditopic asymmetric macrocyclic compounds, with or without pendant arms, may supply well-defined specific environments for the coordination of two metal ions. Additionally it may be possible to tune their physicochemical properties by control of the length and type of bridging groups between the two specific coordination sites.[9,10]

With these applications in mind we have synthesized the new ditopic macrocyclic ligand H_6L^1 {3,7,11-tris-[*N*-(3,4-dihydroxylbenzoyl)-aminopropyl]-3,7,11,17-tetraazabicyclo[11.3.1]heptadeca-1(17),13,15-triene}, see Scheme 1. This ligand offers the amine donors of the 14-membered tetraazamacrocycle for the coordination of copper(II) or zinc(II) and three catecholate units specific for the coordination of iron(III) ions, both sites separated by propyl spacers. The acid–base behaviour of this ligand and its mono-, homo- and heterodinuclear complexes of iron(III), copper(II) and zinc(II) have been studied by several techniques.

[a]*Instituto de Tecnologia Química e Biológica, UNL, Apartado 127, 2781-901, Oeiras, Portugal. E-mail: delgado@itqb.unl.pt; Fax: +351-214 41 12 77; Tel: +351-214 46 97 37/8*
[b]*Instituto Superior Técnico, Av. Rovisco Pais, 1049-001, Lisboa, Portugal*

† Electronic supplementary information (ESI) available: Spectroscopic UV-vis data for the solutions of 1 : 1 and 2 : 1 Cu^{2+} ion to H_6L^1 ratios at different pH values; spectroscopic UV-vis data for Fe^{3+}/H_6L^1 1 : 1 ratio solutions at different pH regions; UV-vis spectroscopic data of $Cu^{2+}/Fe^{3+}/H_6L^1$ 1 : 1 : 1 ratio solutions at different pH; species distribution curves calculated for the Cu^{2+}/H_6L^1 system in aqueous solution; X-band EPR signal of the Fe^{3+}/H_6L^1 1 : 1 ratio solution at pH 10.2. See DOI: 10.1039/b712916e

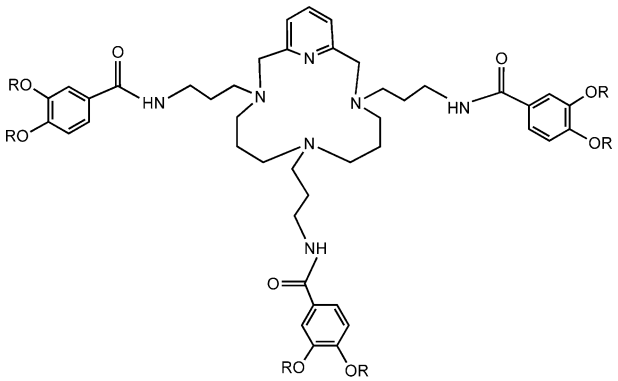

H_6L^1 R = H

L^{1p} R = CH_3

Scheme 1 Molecular structure of H_6L^1 and L^{1p}.

Results and discussions

Synthesis of the macrocyclic compounds

The ligand H_6L^1 was synthesized according to the procedure described by Raymond *et al.*[11,12] for related compounds. Its methyl protected derivative (L^{1p}) was prepared using the Schotten–Baumann technique by addition of 3,4-dimethoxybenzoyl chloride to a mixture of L^{12} (ref. 13) and sodium hydroxide. The selective deprotection of L^{1p} was achieved with BBr_3 in CH_2Cl_2. Upon purification the pure H_6L^1 compound was obtained in good yield as a light beige crystalline powder.

Acid–base behaviour

The protonation constants of the completely deprotonated ligand $(L^1)^{6-}$ were determined from potentiometric measurements in aqueous solution at 298.2 K and ionic strength 0.10 mol dm^{-3} in KNO_3. The determined log K_i^H values ($i = 1$–9) are listed in Table 1 together with the values of related ligands[12,14,15] (see Scheme 2 for the corresponding structures).

In Fig. 1 is shown the species distribution diagram starting from the protonated form of the ligand $(H_9L^1)^{3+}$, obtained with the help of the Hyss program.[16] The compound has ten basic sites, six from the phenolate oxygen atoms of the catecholate groups of the pendant arms and four from the macrocyclic nitrogen atoms. Only six protonation constants could be accurately determined under our experimental conditions. Indeed, the three first protonation constants corresponding to the first deprotonation of each catechol group (very high values) and the last protonation of the macrocyclic ring (very low value) cannot be determined by potentiometry.

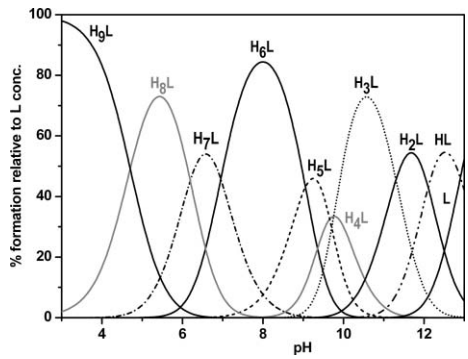

Fig. 1 Species distribution curves calculated for the ligand $(H_9L^1)^{3+}$ in aqueous solution from the protonation constants of Table 1. $C_L = 1.0 \times 10^{-3}$ mol dm^{-3}. L = L^1.

The 2,3-dihydroxybenzene has a very high value for the first protonation constant and a large difference between the intrinsic acidity of the two dissociable protons of the phenolic oxygen atoms (log $K_1 \approx 13$ and log $K_2 = 9.22$).[17] This is explained by electronic effects and intramolecular hydrogen bonding formation between neighbouring protonated and deprotonated phenolic oxygen atoms.[18–21]

The direct determination of the first three protonation constants of $(L^1)^{6-}$ in aqueous solution, corresponding to the first protonation of each catecholate group, is not possible, and was not tried in other solvents owing to solubility reasons. This determination

Table 1 Protonation constants (log K_i^H) of $(L^1)^{6-}$ and of other related compounds for comparison reasons. $T = 298.2$ K and $I = 0.10$ mol dm^{-3} in KNO_3

Reaction Equilibrium	$(L^1)^{6-}$ [a]	$(L^2)^{6-}$ [b]	$(L^3)^{6-}$ [c]	$(L^4)^{6-}$ [d]	$(L^5)^{6-}$ [c]
$(L^1)^{6-} + H^+ \rightleftarrows (HL)^{5-}$	12.9[e]	12.9[e]	12.9[e]	12.9[e]	12.9[e]
$(HL)^{5-} + H^+ \rightleftarrows (H_2L)^{4-}$	12.1[e]	12.1[e]	12.1[e]	12.1[e]	12.1[e]
$(H_2L)^{4-} + H^+ \rightleftarrows (H_3L)^{3-}$	11.3[e]	11.26	11.3[e]	11.3[e]	11.3[e]
$(H_3L)^{3-} + H^+ \rightleftarrows (H_4L)^{2-}$	9.76(5)	8.75	8.55	9.26	8.4
$(H_4L)^{2-} + H^+ \rightleftarrows (H_5L)^{-}$	9.65(4)	8.61	7.5	8.65	7.4
$(H_5L)^{-} + H^+ \rightleftarrows H_6L$	9.05(3)	6.71	6.0	7.86	5.9
$H_6L + H^+ \rightleftarrows (H_7L)^+$	6.95(5)	5.88	—	—	—
$(H_7L)^+ + H^+ \rightleftarrows (H_8L)^{2+}$	6.19(5)	—	—	—	—
$(H_8L)^{2+} + H^+ \rightleftarrows (H_9L)^{3+}$	4.70(5)	—	—	—	—
$(L^1)^{6-} + 6\,H^+ \rightleftarrows (H_6L)$	64.8	60.3	58.4	62.1	58.0
$(L^1)^{6-} + 7\,H^+ \rightleftarrows (H_7L)^+$	71.7	66.2	—	—	—
$(L^1)^{6-} + 9\,H^+ \rightleftarrows (H_9L)^{3+}$	82.6	—	—	—	—
	7.40[f]	7.49[g]	7.36[g]	8.59[g]	7.2[g]

[a] This work. [b] Ref. 12. [c] $I = 0.1$ mol dm^{-3} KCl, 5% CH_3OH, ref. 14. [d] Ref. 15. [e] Estimated values. [f] Average log K_i^H of the three more acidic catecholamide protonation constants: $\sum(\log K_6 + \log K_7 + \log K_8)/3$. [g] See footnote (f), but the corresponding constants are K_4, K_5 and K_6: $\sum(\log K_4 + \log K_5 + \log K_6)/3$.

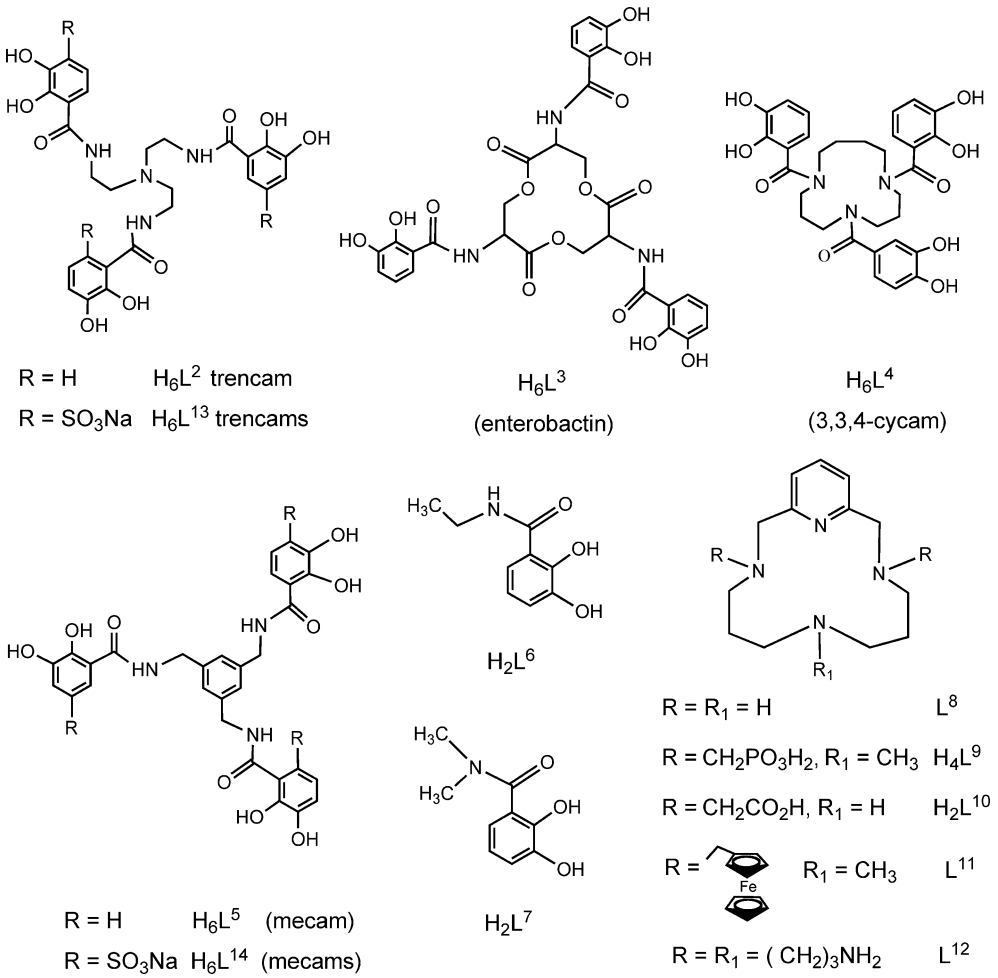

Scheme 2 Molecular structure of related compounds.

is not only difficult because of the very high values, but also due to the possible oxidation of the ligand at pH ≈ 12, as observed for other catecholamide derivatives.[22] These values are around 13 for the tris- and bis-catecholate compounds.[14,15,19,20] Taking this into account and the ineluctable statistical factor, and according to usual practice[12,19] we have estimated for these constants the values of log $K_1^H = 12.9$, log $K_2^H = 12.1$ and log $K_3^H = 11.3$, see Table 1.

The titration curve of $(H_9L^1)^{3+}$ contains three buffer regions. The first region at pH 4 to 5 corresponds to the titration of one proton of one ammonium centre of the macrocycle,[23] the second one at pH 6 to 9 is a well defined region of two protons of catecholate groups, and the last one above pH 9 corresponds to the titration of the remaining six protons. At pH 8 about 90% of the ligand is in the zwitterionic form H_6L^1 (see Fig. 1), having the two nitrogen atoms contiguous to the pyridine of the macrocycle protonated and the catecholate arms bound to these ammonium groups with only one proton, each one with one negative charge, and the remaining arm completely protonated. The sequence of protonation is straightforward taking into account the acid–base behaviour of the parent macrocycle (L^8),[23] and ligands containing or not tertiary amines coupled with catecholamide groups, such as mecam,[14] and trencam.[12]

The quite high values of K_4^H and K_5^H of the ligand when compared with those of the parent macrocycle can be explained by electronic effects due to the formation of the zwitterionic species and/or additional stabilization by hydrogen bonds. The values of K_6^H–K_8^H are ascribed to the three consecutive protonations of the less basic oxygen atoms of the catecholamide dianions closer to the amide carbonyl function. The average value for these three constants is comparable to the corresponding value for trencam,[12] enterobacin,[14] and for other catecholamide ligands[20] (see Table 1), in good agreement with the value of log K_2^H = 7.34 for H_2L^6.[24] On the other hand, the average value of the three more acidic protonation constants of 3,3,4-cycam[15] is 8.59, which is similar to that of H_2L^7,[25] (see Table 1 and Scheme 2). In fact, theoretical calculations, together with the crystal structures and experimental potentiometric data for a series of catecholamide derivatives established that the presence of amide nitrogen atoms on the catecholamide molecule increases the first protonation constant of the nearby catecholate by about one log unit.[21] Finally, it can be seen that the difference between consecutive log K values of $(L^1)^{6-}$ are larger than the expected statistical separation (log 3 or 0.48), which points to interactions between the catecholate oxygen atoms in the pendant arms.[20]

Metal complex studies

Mono- and homodinuclear complexes

The stability constants of complexes of $(H_9L^1)^{3+}$ with Fe^{3+}, Cu^{2+} and Zn^{2+} metal ions were determined under the experimental conditions indicated above, and the values are listed in Table 2. The constants were determined for the entire pH range starting from the ligand in the form $(H_9L^1)^{3+}$, however the ligand will be indicated in the following text by the neutral form H_6L^1.

Table 2 Overall ($\log \beta_{M_mH_hL^1}$) and stepwise ($\log K_{M_mH_hL^1}$) stability constants of complexes of H_6L^1 with M = Fe^{3+}, Cu^{2+} and Zn^{2+} [a]

	Fe^{3+}	Cu^{2+}	Zn^{2+}
Equilibrium reaction[b]	$\log \beta_{M_mH_hL^1}$		
$M + L^1 \rightleftarrows ML^1$	43.38(9)	—	—
$M + H + L^1 \rightleftarrows MHL^1$	53.11(8)	39.19(9)	27.7(1)
$M + 2\,H + L^1 \rightleftarrows MH_2L^1$	61.54(7)	49.59(9)	38.84(7)
$M + 3\,H + L^1 \rightleftarrows MH_3L^1$	68.48(5)	59.16(8)	48.82(6)
$M + 4\,H + L^1 \rightleftarrows MH_4L^1$	73.46(4)	67.18(8)	57.44(5)
$M + 5\,H + L^1 \rightleftarrows MH_5L^1$	76.77(2)	73.38(3)	64.34(2)
$M + 6\,H + L^1 \rightleftarrows MH_6L^1$	79.40(5)	77.82(1)	69.75(6)
$2\,M + L^1 \rightleftarrows M_2L^1$	65.25(6)	47.83(6)	—
$2\,M + H + L^1 \rightleftarrows M_2HL^1$	69.78(5)	57.04(4)	38.50(7)
$2\,M + 2\,H + L^1 \rightleftarrows M_2H_2L^1$	—	62.73(3)	47.62(3)
$2\,M + 3\,H + L^1 \rightleftarrows M_2H_3L^1$	—	67.26(6)	54.88(3)
$2\,M + L^1 + H_2O \rightleftarrows M_2L^1(OH) + H$	57.79(8)	—	—
$2\,M + L^1 + 2\,H_2O \rightleftarrows M_2L^1(OH)_2 + 2\,H$	49.00(8)	—	—
$2\,M + L^1 + 3\,H_2O \rightleftarrows M_2L^1(OH)_3 + 3\,H$	38.90(9)	—	—
	$\log K_{M_mH_hL^1}$		
$M + L^1 \rightleftarrows ML^1$	43.38	—	—
$ML^1 + H \rightleftarrows MHL^1$	9.73	—	—
$MHL^1 + H \rightleftarrows MH_2L^1$	8.43	10.40	11.15
$MH_2L^1 + H \rightleftarrows MH_3L^1$	6.94	9.57	9.98
$MH_3L^1 + H \rightleftarrows MH_4L^1$	4.98	8.02	8.62
$MH_4L^1 + H \rightleftarrows MH_5L^1$	3.31	6.20	6.90
$MH_5L^1 + H \rightleftarrows MH_6L^1$	2.63	4.44	5.41
$ML^1 + M \rightleftarrows M_2L^1$	21.87	—	—
$M_2L^1 + H \rightleftarrows M_2HL^1$	4.53	9.21	—
$M_2HL^1 + H \rightleftarrows M_2H_2L^1$	—	5.69	9.12
$M_2H_2L^1 + H \rightleftarrows M_2H_3L^1$	—	4.53	7.26
$M_2L^1(OH) + H \rightleftarrows M_2L^1$	7.46	—	—
$M_2L^1(OH)_2 + H \rightleftarrows M_2L^1(OH)$	8.79	—	—
$M_2L^1(OH)_3 + H \rightleftarrows M_2L^1(OH)_2$	10.10	—	—

[a] $T = 298.2$ K and $I = 0.10$ mol dm^{-3} KNO_3. [b] The charges of species were omitted for simplicity reasons, due to the fact that metal ions of different charges are considered.

Mononuclear and dinuclear complexes were found under our experimental conditions. Hydroxocomplexes, $[M_2H_{-h}L^1]^{-h}$ (h = 1–3), were only observed for M = Fe^{3+}.

The potentiometric titration curves of the metal ion to H_6L^1 1 : 1 ratio solutions with strong base display a plateau in the pH 4–5 region and then a gradual increase of pH, indicating the successive deprotonation of complexes. Along the titration, in the case of the Fe^{3+} ion, the colour of the solution changes from blue to blue green (pH 2–4), light to dark purple (pH 4.5–8.5) and red wine to dark red (pH > 11), while the Cu^{2+} solutions change from light blue to greenish blue (pH 3.1–6.5) and greenish yellow to bright yellow (pH 7 to >10.5). In the curves of the 2 : 1 solutions the plateau region extends for 3 more equiv. of base.

Six different mono $[FeH_{h-1}L^1]^{h-3}$ and one dinuclear protonated $[Fe_2HL^1]^+$ species can be formed, but only dinuclear complexes exist for the 2 : 1 ratio, as shown in the distribution curves of Fig. 2. At pH 6–7, the $[Fe_2L^1]$ complex exists at 90% of the total metal concentration, and then at higher pH values hydroxo complexes are formed. The latter species derive from the hydrolysis of water molecules directly bound to the metal, these water molecules should complete the coordination sphere of the metal coordinated to the macrocyclic amines. The dinuclear complexes may contain one metal coordinated to the amine donors of the macrocycle and the other one coordinated to the catecholate oxygen donors of the arms. In fact, due to the 3,4-dihydroxybenzoyl position of the arms in the ligand, the iron(III) coordination sphere is not of the "salicylate" type,[26] the metal coordination to the carbonyl oxygen atoms is prevented due to conformational limitation of the ligand.[19,27]

The deprotonation of the last two protons from $[MH_2L^1]^{2-}$ (M = Cu^{2+} or Zn^{2+}) complexes, is only achieved at very high pH, and the corresponding constants were not determined by the reasons already discussed for the first three protonation constants of the ligand. This fact indicates that these protons are located at the catecholate arms, the corresponding constants should be only slightly lower than the first two protonation constants of the free ligand due to the presence of the metal centre, suggesting that these metal ions prefer the macrocyclic environment when only 1 equiv. of metal ion is added, or that one of the arms is not involved in the coordination of the second metal ion.

The distribution diagram curves of Cu^{2+}/H_6L^1 2 : 1 ratio (see Fig. S1 in ESI†) show successively the formation of $[Cu_2H_2L^1]$

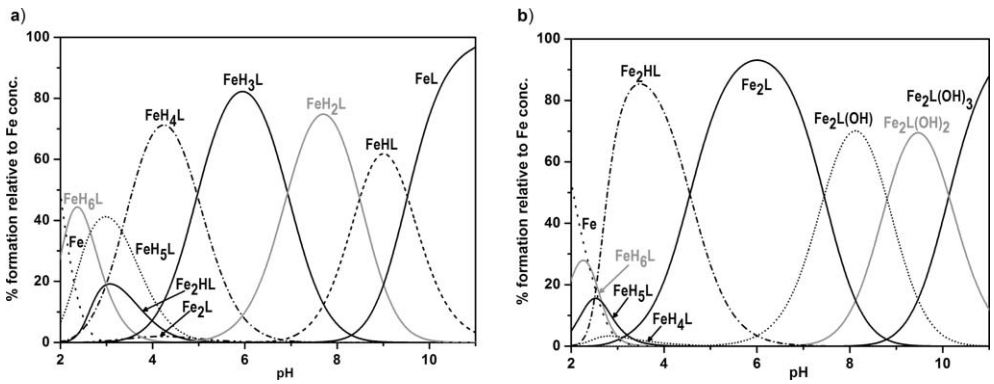

Fig. 2 Species distribution curves calculated for the Fe^{3+}/H_6L^1 system in aqueous solution. (a) $C_{Fe} = C_L = 1.0 \times 10^{-3}$ mol dm^{-3} and (b) $C_{Fe} = 2 \times C_L = 2.0 \times 10^{-3}$ mol dm^{-3}. L = L^1.

Table 3 The pFe values for Fe^{3+} complexes of H_6L^1 and related ligands at pH = 7.4[a]

Chelator[b]	pFe	Ref.
H_6L^1	27.34	This work
Enterobactin	35.5	19
mecam	29.1	15
trencam	27.8	12
Desferrioxamine B	26.6	25
Transferrin	23.6	25
3,3,4-cycam	23.0	15

[a] $C_{Fe} = 10^{-6}$ mol dm^{-3}, $C_L = 10^{-5}$ mol dm^{-3}. [b] H_6L^1 is written in the neutral form while the other chelators are designated by their traditional names.

(≈60% at pH 6), $[Cu_2HL^1]^-$ (100% at pH 8.5) and then starts to form $[Cu_2L^1]^{2-}$ complexes. At pH < 6 mononuclear protonated species also exist.

The binding affinity of H_6L^1 for Zn^{2+} is much lower than for Cu^{2+}, the complexes start to form at pH ≈ 5, and for 2 : 1 ratio solutions $Zn(OH)_2$ is formed at pH ≈ 10 precluding the determination of the stability constant of the $[Zn_2L^1]^{2-}$ complex.

The stability constant of $[FeL^1]^{3-}$ and the overall basicity of the ligand are both very large. In order to compare the iron(III) binding properties of H_6L^1 with other iron(III) chelators, the different proton competitions should be taken into account, for instance by the calculation of pFe (= −log [Fe^{3+}]) at a given pH.[16] In Table 3, the pFe values determined for solutions of iron(III) complexes of several chelators at pH 7.4 were compiled. At this pH, the pFe value of the ferric complex of H_6L^1 is slightly lower than that of enterobactin,[19] but it is still among the values of those of the most effective catecholate iron(III) chelators, such as mecam[15] and trencam.[12] On the other hand, the pFe for H_6L^1 is higher than that of the plasma-iron transport protein, transferrin,[25] indicating that H_6L^1 may take the iron from transferrin and facilitate its excretion from the body. Additionally, the pFe value for our ligand is also higher than those of 3,3,4-cycam[15] or desferrioxamine B.[25]

The H_6L^1 ligand was not designated for the specific coordination of iron(III), but instead for the study of heterodinuclear complexes, even so the results have shown that it is one of the best chelators for this metal ion. In fact the chelator should adopt an arrangement with the three long aminopropyl arms located at the same side of the macrocyclic plane[13] forming a tripodal configuration and the amide functions located out of the catecholate oxygen atom's network. This preorganized arrangement should favour metal complexation.

Studies of chelators with catecholate substituents with copper(II) or zinc(II) are very rare in the literature. Table 4 lists the pM values for H_6L^1 and other related ligands for M = Cu^{2+} or Zn^{2+} ions at pH 7.4.[23,28–31] The pCu value at physiological pH for H_6L^1 is very similar to that for other N-derivatives of the parent macrocyclic ligand, such as H_4L^9,[28] and H_2L^{10}.[30] However, the pCu values are also of the same order as those for typical catecholamide ligands, such as H_6L^{13} (trencams)[31] and H_6L^{14} (mecams),[29] see Table 4. Copper(II) complexed with H_2L^{10} exhibits a distorted octahedral environment with the four macrocyclic nitrogen atoms forming the equatorial plane and two oxygen atoms from the methylcarboxylate arms in axial positions,[30] while in the complex with the tris-catecholate ligand H_6L^{13} (trencams) the copper is coordinated in bis-catecholate fashion.[31] These results indicate that the two types of coordination of copper(II) afford comparable binding affinities at physiological pH, and therefore we cannot determine whether the metal is coordinated at the arms or at the macrocycle, and probably an equilibrium between both types of coordination should exist. On the other hand, the relatively low pZn value for H_6L^1/Zn^{2+} indicates that the structure of H_6L^1 does not favour the effective coordination of Zn^{2+}.

Table 4 The pM values for M = Cu^{2+} and Zn^{2+} complexes of H_6L^1 and related ligands at pH = 7.4[a]

Chelator	pCu	pZn	Ref.
H_6L^1	18.15	8.44	This work
H_4L^9	16.21	14.34	28
H_6L^{14} (mecams)	16.9	11.3	29
L^8	17.00	13.34	23
H_2L^{10}	18.85	13.13	30
H_6L^{13} (trencams)	18.9	11.7	31

[a] $C_M = 10^{-6}$ mol dm^{-3}, $C_L = 10^{-5}$ mol dm^{-3}.

Cu^{2+}/Fe^{3+} and Cu^{2+}/Zn^{2+} heterodinuclear complexes

The formation of heterodinuclear complexes is expected to be due to the presence of two different coordination sites in the molecule of H_6L^1 and the observed tendency of this chelator to form dinuclear complexes. The stability constants of the heterodinuclear complexes of H_6L^1 with Cu^{2+}/Fe^{3+}, and Cu^{2+}/Zn^{2+} were determined, and the values are listed in Table 5.

The potentiometric titration curves of Cu^{2+} : Fe^{3+} : H_6L^1 (or Cu^{2+} : Zn^{2+} : H_6L^1) 1 : 1 : 1 molar ratio show the break upon addition of nine (or eight) equivalents of base. Eight equivalents for the second system because the deprotonation of the last proton of $[CuZnHL^1]^-$ occurs at pH ≈ 9.5, see Table 5. The colour of the $Cu^{2+}/Fe^{3+}/H_6L^1$ (1 : 1 : 1) solution changes during the titration from intense blue-green at low pH to red-purple (pH 4.0–8.0), and dark red purple at high pH, significantly different from the colour of solutions with only one metal ion.

The species distribution diagram for the $Cu^{2+}/Fe^{3+}/H_6L^1$ system is shown in Fig. 3. Mononuclear $[FeH_hL^1]^{h-3}$ (h = 5, 6) species are formed simultaneously with $[CuFeH_hL^1]^{h-1}$ (h = 2, 3) complexes at pH 2–4. At pH > 4 only heterodinuclear $(CuFeH_hL^1)^{h-1}$ (h = 0, 1) complexes exist in solution. At physiological pH the $[CuFeL^1]^-$ complex exists at more than 95% of the total ligand

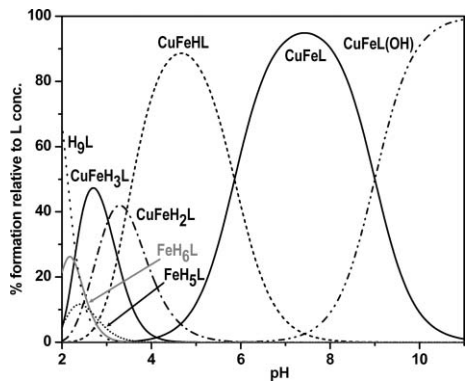

Fig. 3 Species distribution curves calculated for the heterodinuclear $Cu^{2+}/Fe^{3+}/H_6L^1$ systems in aqueous solution ($C_{Cu} = C_{Fe} = C_L = 1.0 \times 10^{-3}$ mol dm^{-3}). L = L^1.

Table 5 Overall ($\log \beta_{MM'H_hL}$) and stepwise ($\log K_{MM'H_hL}$) stability constants of heterodinuclear complexes of H_6L^1 with $M/M' = Cu^{2+}/Fe^{3+}$ and Cu^{2+}/Zn^{2+}. $T = 298.2$ K and $I = 0.10$ mol dm^{-3} KNO_3

	$\log \beta_{MM'H_hL}$	
Reaction equilibrium	$M = Cu^{2+}$; $M' = Fe^{3+}$	$M = Cu^{2+}$; $M' = Zn^{2+}$
$M + M' + L^1 \rightleftarrows MM'L^1$	63.40(7)	41.6(1)
$M + M' + H + L^1 \rightleftarrows MM'HL^1$	69.26(4)	51.22(9)
$M + M' + 2\,H + L^1 \rightleftarrows MM'H_2L^1$	72.71(3)	58.86(7)
$M + M' + 3\,H + L^1 \rightleftarrows MM'H_3L^1$	75.74(2)	65.26(9)
$M + M' + 4\,H + L^1 \rightleftarrows MM'H_4L^1$	—	71.3(1)
$M + M' + L^1 \rightleftarrows MM'L^1(OH) + H$	54.40(9)	—
	$\log K_{MM'H_hL}$	
$ML^1 + M' \rightleftarrows MM'L^1$	36.2[a]	—
$M'L^1 + M \rightleftarrows MM'L^1$	20.02	—
$MM'L^1 + H \rightleftarrows MM'HL^1$	5.86	9.59
$MM'HL^1 + H \rightleftarrows MM'H_2L^1$	3.45	7.64
$MM'H_2L^1 + H \rightleftarrows MM'H_3L^1$	3.03	6.40
$MM'H_3L^1 + H \rightleftarrows MM'H_4L^1$	—	6.0
$MM'L^1(OH) + H \rightleftarrows MM'L^1$	9.00	—

[a] Determined taking the value of $\log K_{CuL^1} = 27.19$ obtained by estimation of $\log K_{CuHL^1} = 12.0$, which is a very realistic value, see text.

concentration and at pH ≈ 7.5 the $[CuFeL^1(OH)]^{2-}$ complex starts to form. The formation of protonated mononuclear iron(III) complexes at very low pH reveals that the iron(III) coordinates to the catecholate oxygen atoms, being the most thermodynamically stable species formed and then the copper(II) ion coordinates to the remaining sites of the ligand, which are the donor atoms of the macrocyclic ring. The formation of $[CuFeL^1(OH)]^{2-}$ at high pH values implies the presence of one water molecule in one of the metal coordination spheres. The pCu and pFe values determined at pH 7.4 for this system are 18.10 and 27.30, respectively. These values are very close to the corresponding ones for each metal ion determined independently (see Tables 3 and 4), which attest to the weak interaction between both centres.

The distribution curves diagrams for a 1:1:1 ratio of $Cu^{2+}/Zn^{2+}/H_6L^1$ shows a similar behaviour, but in this case it is not possible to assign a specific site to each metal ion. At low pH values (< 4) the copper(II) complexes are formed while the catecholate groups are still protonated and then the zinc(II) coordinates to some of the free binding sites of the ligand. At pH 10 the $[CuZnL^1]^{2-}$ complex is formed at 80% of the total ligand concentration, and the $[CuZnL^1(OH)]^{-}$ complex is formed at high pH values. It is also interesting to note that the stability constants determined are consistent with formation of heterodinuclear complexes and that homodinuclear complexes are not formed over the entire pH range.

The rationalization of the coordination behaviour of H_6L^1 with the studied metal ions based only on the potentiometric data are not completely certain, but some comments can be advanced. The ditopic ligand H_6L^1 strongly binds Fe^{3+} and Cu^{2+} simultaneously, each metal in a different coordination site of the ligand forming the heterodinuclear complex. The tendency to form other types of coordination, means that the Fe^{3+} coordinated in the macrocyclic nitrogen atoms and the Cu^{2+} in the bis-catecholate mode, should also favour homodinuclear species formation, and this did not occur. It is known that iron(III) has a very high affinity for the negative catecholate groups. However, the coordination of iron(III) to the arms of the ligand probably imposes a special arrangement of the macrocyclic cavity. Therefore a geometric arrangement is necessary for the final coordination of the copper ion. This geometric reorganization appeared to be thermodynamically favoured. For the $[CuZnL^1]^{2-}$ complex, in spite of the non-specific tendency of Zn^{2+} to catechol coordination, the formation of the heterodinuclear species is also favoured, and in this case again homodinuclear species are not formed (Fig. 4). In conclusion the ligand H_6L^1 is able to coordinate simultaneously two different metal ions at its different binding sites forming $[CuFeL^1]^{-}$ and $[CuZnL^1]^{2-}$ heterodinuclear complexes, which are thermodynamically stable species at physiological pH. Accordingly, this ligand can be explored for mimetic models of heterodinuclear protein sites of cytochrome a oxidase[32] and Cu/Zn SOD enzymes, which catalyse the dismutation of the superoxide anion and play an important role in the protection of cells from oxidative damage.[33]

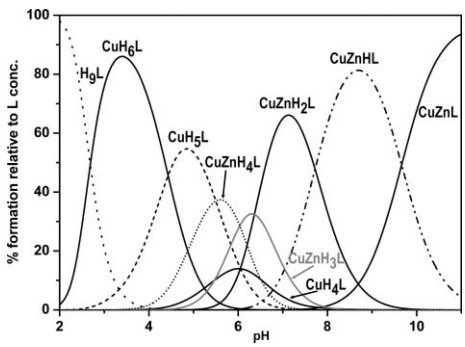

Fig. 4 Species distribution curves calculated for the heterodinuclear $Cu^{2+}/Zn^{2+}/H_6L^1$ systems in aqueous solution ($C_{Cu} = C_{Zn} = C_L = 1.0 \times 10^{-3}$ mol dm^{-3}). $L = L^1$.

UV-vis and EPR spectroscopic studies

Copper(II) complexes

UV-vis spectra of Cu^{2+} to H_6L^1 solutions, 1:1 and 2:1 ratios, were recorded in the pH 5.4–10 range. The data are listed in ESI

Table S1† and the UV region of some spectra is shown in Fig. 5. All the spectra show a broad asymmetric band at 626 nm with shoulders at 430, 550 and 740 nm due to the copper d–d transition. The molar absorptivities (ε/dm^3 mol^{-1} cm^{-1}) of all of them steadily increase with an increase in pH. In the UV region the bands of the ligand at 256 and 290 nm shift to 250 and 316 nm (with a shoulder at 326 nm) with copper(II) complex formation in the pH 3–7 range. Although the ligand bands shift to 275 and 305 nm at pH > 8, the bands of the complex keep the same position but with increasing intensities (see Table S1†). The 2 : 1 ratio solutions present the same bands but larger molar absorptivities compared to the 1 : 1 ratio solutions, having almost double intensities at pH 9.1. The shoulders at 430 and 550 nm are assigned to catecholate to copper charge transfer bands, and they are indicative of the binding of the catecholate oxygen atoms of H_6L^1 to the copper(II) centre, together with the bands in the UV region. The same features were also found in copper complexes of other catecholate ligands.[4,34,35]

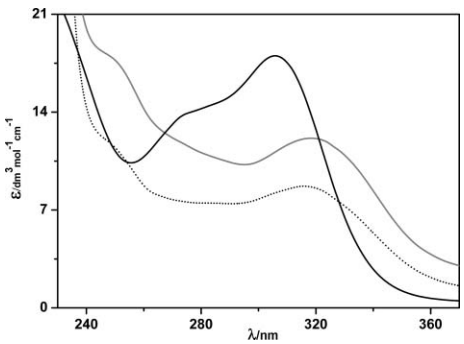

Fig. 5 Absorption spectra of the H_6L^1 free ligand (pH 9.7, black line) and its 1 : 1 (pH 10.0, dot line) and 2 : 1 (pH 9.1, gray line) copper complexes in the UV region. The *Y*-axis is multiplied by the factor 10^{-3}.

The X-band EPR spectra of the Cu^{2+}/H_6L^1 1 : 1 ratio aqueous solutions at pH 5.6 and 10, taken at 13 and 5 K, respectively, are very similar, exhibiting three well resolved lines of the four expected at low field arising from coupling of the unpaired electron spin with the copper nucleus and no superhyperfine splitting was due to coupling with nitrogen atoms. The fourth copper line is partially overlapped by the strong and not resolved line of the high field part of the spectra, see Fig. 6(a). The hyperfine coupling constants (A) and g values obtained by the simulation of the spectra[36] are compiled in Table 6 together with those of other copper(II) complexes having the same macrocyclic framework but different arms.[30,37,38]

The simulations of the EPR spectra of both 1 : 1 ratio Cu^{2+}/H_6L^1 solutions led to three different g values with $g_z > (g_x + g_y)/2$, which is typical of the tetragonal copper(II) ion in rhombic symmetry

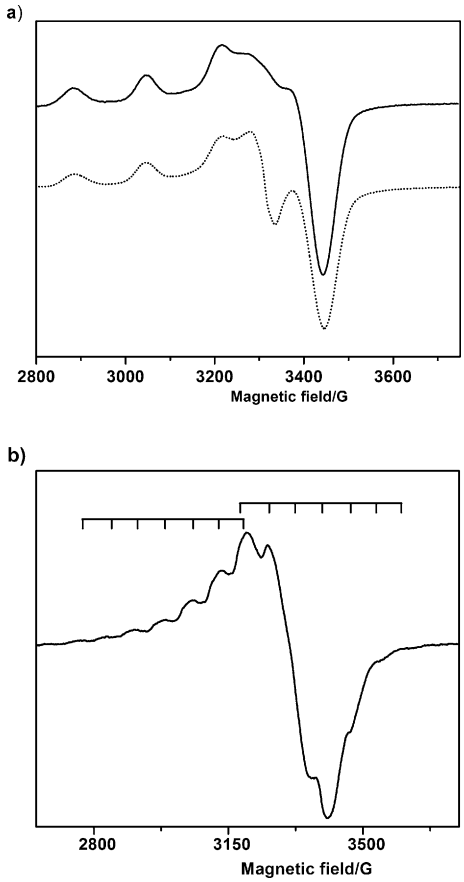

Fig. 6 X-Band EPR spectra of Cu^{2+}/H_6L^1 solutions: (a) 1 : 1 ratio at pH = 5.6 (dot line) and 10 (solid line), recorded at 13 and 5 K, respectively, microwave power of 2.4 mW, and (b) 2 : 1 ratio at pH = 12, recorded at 5 K, microwave power of 2.35 mW. All spectra acquired in water–DMSO (1 : 1 v/v), modulation amplitude of 1 mT and frequency of 9.644 GHz.

and $d_{x^2-y^2}$ ground state.[30,37,39,40] The g_i and A_i ($i = x$, y and z) values should be related to the strength of the axial donor and the displacement of the copper(II) ion from the donor atom plane as derived from ligand-field theory.[39,40]

In agreement, the coordination of axial ligands to the square-planar geometry of $[CuL^8]^{2+}$[38,40] has the effect of decreasing A_z and increasing g_z with a simultaneous red shift in λ_{max}, as observed in $[CuL^{11}Cl]^+$[37] and $[CuL^{10}]$[30] where the metal centres adopt a distorted square pyramidal and an octahedral geometry, respectively, the macrocyclic nitrogen atoms forming the equatorial plane. Therefore the EPR parameters of the copper(II) complexes of Cu^{2+}/H_6L^1 1 : 1 ratio solutions are consistent with distorted square pyramidal (at pH 5.6) and, probably, octahedral (at pH 10.0)

Table 6 X-Band EPR data for Cu^{2+}/H_6L^1 1 : 1 ratio solutions at pH 5.6 and 10, and for other related complexes

		EPR parameters (10^4 A_i/cm^{-1}); g_z/A_z/cm							
Copper(II) complexes	λ_{max}/nm	g_x	g_y	g_z	A_x	A_y	A_z	g_z/A_z	Ref.
Cu^{2+}/H_6L^1 (pH 5.6)	632	2.031	2.086	2.198	6.4	11.3	173.6	126	This work
Cu^{2+}/H_6L^1 (pH 10)	632	2.040	2.074	2.202	24.7	22.2	166.3	132	This work
$[CuL^{11}Cl]^+$	600	2.032	2.074	2.199	0.8	17.2	170.3	129	37
$[CuL^{10}]$	614	2.034	2.08	2.209	14.3	8.5	167.1	132	30
$[CuL^8]^{2+}$	560	2.034	2.060	2.188	0.5	3.4	192.9	113	38

geometries for the copper(II) centre. The empirical value g_z/A_z, which is almost equal for all the complexes in Table 6, except for $[CuL^8]^{2+}$, is also indicative of their structural similarity.[41]

The EPR spectrum of the Cu^{2+}/H_6L^1 2:1 ratio solutions at pH 12, where the $[Cu_2L^1]^{2-}$ complex is formed at 100%, is indicative of dinuclear copper(II) species in a paramagnetic triplet spin state, see Fig. 6(b). The parallel hyperfine pattern shows seven regular well resolved lines in the $\Delta M_s = \pm 1$ transition.[42–45] If the unpaired electrons of the two copper nuclei with individual $S = 1/2$ are coupled ($I_{Cu} = 3/2$), each of the two resonances will exhibit seven-line copper hyperfine patterns, $(2I_n + 1)$.[45] Therefore it is expected that the two septets shift in respect to each other by zero-field splitting, $2D$.[42,43] In the $[Cu_2L^1]^{2-}$ spectrum, the well defined seven-lines have a coupling constant $A_{\parallel}$ of 70.7 G, a value that is about one-half of the equivalent value for mononuclear copper(II) complexes, indicating also that a metal–metal interaction occurs.[42,46] No superhyperfine splitting due to the coupling with the nitrogen atoms of the macrocycle was observed, which is common in copper(II) macrocyclic complexes.[28,30,37,38] The $\Delta M_s = \pm 2$ transition signal was not observed. When the coupling between the metal centres is weak the signal in the half-field can be indiscernible, which have been observed for varied copper(II) dinuclear complexes.[47–49]

From the D value it is possible to determine the mean distance between the two copper centres, when the zero-field splitting parameter is due to a pure dipole–dipole interaction.[42–44,47] In this case the effective dipolar zero-field splitting is proportional to $1/r^3$ (r being the distance between the two copper(II) centres) by the equation: $D_{\parallel} = 0.65(g_{\parallel})^2/r^3$.[42,44,48] The calculated values for $[Cu_2L^1]^{2-}$ complex are: $D_{\parallel} = 0.02062$ cm^{-1} and $r = 4.87$ Å. These values should only be considered as tentative,[42,46,50] but they are indicative of a weak interaction between the two copper(II) centres.

Fe^{3+} complexes

The UV-vis spectra of the aqueous solutions of Fe^{3+}/H_6L^1 1:1 ratio were recorded at different pH and are shown in Fig. 7, and the respective data are presented in Table S2.†

Two or more species coexists at each pH value till 11, see Fig. 2 (a): $[FeH_4L^1]^+$ and $[FeH_3L^1]$ at pH 5.0; $[FeH_3L^1]$ and $[FeH_2L^1]^-$ at pH 6.9, respectively. At pH 11.4 the $[FeL^1]^{3-}$ complex is the unique species in solution, which exhibits a characteristic red colour and intense band at 474 nm ($\varepsilon = 4800$ dm^3 mol^{-1} cm^{-1}), which arise from ligand to metal d transitions.[51]

In the UV region the absorption maxima of the free H_6L^1 (pH 10) at 275 and 305 nm shift to 250 and 316 nm, respectively, which is indicative of the formation of the iron(III) tris-catecholate complex.[51] Similar bands were observed with the biological substrate of 1,2-catechol dehydrogenase, an intradiol enzyme that coordinates iron(III) as its catecholate dianion.[52]

The EPR spectrum of the ferric/H_6L^1 1:1 ratio aqueous solution was recorded at 4.7 K and pH 10.2. At this pH value the $[FeL^1]^{3-}$ complex is present in 90% of the total metal concentration. The spectrum shows an intense isotropic signal at $g \approx 4.27$ of the transition between the middle Kramer's doublet, and a broad peak at $g \approx 9.6$ from the ground state doublet of a rhombic distorted iron(III) ion in high-spin state ($S = 5/2$) with $E/D \approx 0.31$, Fig. S3, in ESI.† The signal is sharp (line width is 10 G) and no splitting was observed, which is indicative of homogenous environment around the metal centre. These features are typical of ferric centres in a tris-catecholate environment.[53,54] The high intensity of the signal is characteristic of the tris-catecholate mode of bonding, corresponding to the formation of a trigonal distorted octahedral geometry.[54]

$[CuFeH_hL^1]^{h-1}$ complexes

The spectroscopic UV-vis data of $Cu^{2+}/Fe^{3+}/H_6L^1$ 1:1:1 ratio aqueous solutions recorded at pH 7.0 and 10.0 are listed in Table S3, ESI,† and in Fig. 8 are shown the spectrum at pH 10.0 together with those of Fe^{3+}/H_6L^1 1:1 and Cu^{2+}/H_6L^1 solutions at pH 11.4 and 10.0, respectively. Following the speciation diagram of Fig. 3, the $[CuFeL^1]^-$ and $[CuFeL^1(OH)]^{2-}$ complexes are presented at about 100% of the total ligand amount at pH ≈ 7 and 10, respectively.

The band at 474 nm of $[FeL^1]^{3-}$ shift to 454 nm for the heterodinuclear species and the corresponding ε value is about half of that for the LMCT catecholate to iron(III) band of the $[FeL^1]^{3-}$ complex. The copper d–d transition band of the heterodinuclear complex is hidden by the intense iron(III)/copper(II) catecholate charge transfer band. The UV spectra of $Cu^{2+}/Fe^{3+}/H_6L^1$ 1:1:1 ratio solutions also exhibit shoulders at 406 nm (pH 7.0) or 370 nm (pH 10).

In conclusion, the observed bands of the heterodinuclear complex are shifted relatively to the corresponding ligand bands, and on the other hand, also move compared to the bands of mononuclear iron(III) and copper(II) species, see Table S1–S3 in ESI† and Fig. 5, 7 and 8.

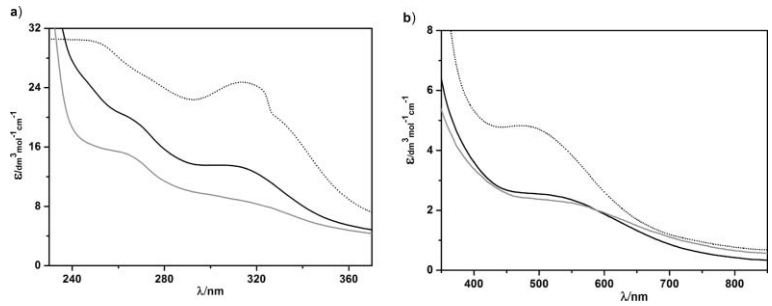

Fig. 7 Absorption spectra of the UV (a) and visible (b) regions of Fe^{3+}/H_6L^1 1:1 ratio aqueous solutions at different pH: 5.0 (grey line), 6.9 (black line), 11.4 (dot line). The Y-axis is multiplied by the factor 10^{-3}.

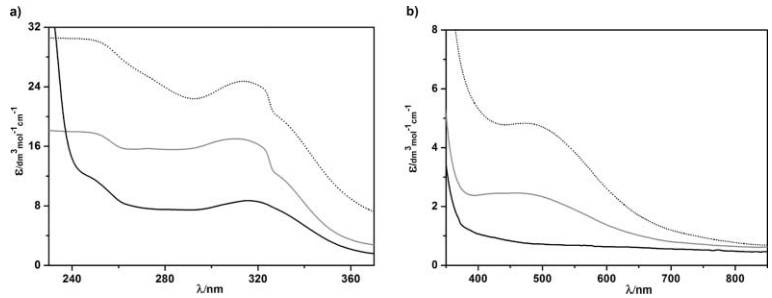

Fig. 8 UV (a) and vis (b) spectra of $Cu^{2+}/Fe^{3+}/H_6L^1$ 1 : 1 : 1 ratio at pH 10.0 (grey line), Fe^{3+}/H_6L^1 1 : 1 ratio at pH 11.4 (dot line), and Cu^{2+}/H_6L^1 1 : 1 at pH 10.0 (black line) aqueous solutions. The *Y*-axis is multiplied by a factor 10^{-3}.

The EPR spectra of the $Cu^{2+}/Fe^{3+}/H_6L^1$ 1 : 1 : 1 ratio aqueous solutions at 5 K and at pH 4.6 and 10.2, are shown in Fig. 9. These solutions contain 90% of $[CuFeHL^1]$ and about 100% of $[CuFeL^1]^-$ complexes of the total amount of ligand, respectively (Fig. 3). Both spectra exhibit two types of signal, one at lower field assigned to a rhombic distorted iron(III) complex in high-spin state d^5 state ($S = 5/2$), and the other of the $\Delta M_s = \pm 1$ transition ($g \approx 2$) showed a hyperfine pattern comparable to that observed for the $[Cu_2L^1]^{2-}$ complex at pH 12, Fig. 6b.

Using the spin-Hamiltonian formalism for the high-spin d^5 state of iron(III),[55] the lower field resonances of the spectra of the solution at pH 4.6 can be assigned to two iron(III) species with rhombic distortion E/D of 0.126 and 0.278, respectively. The solution at pH = 10.2 can be attributed to a species with different rhombic distortion of 0.288.[53,54] The effective *g* values expected for each Kramers doublet are indicated in Table 7, and the signals observed in the spectra are in italics.

The presence of two types of high-spin species of different E/D at pH 4.6 arises from the possible formation of a bis-catecholate together with a small percentage of a tris-catecholate environment around the iron(III) centre. Indeed the E/D value increases with increasing number of catecholate oxygen atoms in the iron(III) coordination sphere, the existence of single species, as found at pH 10.2, with $E/D \approx 0.3$ is predicted for the trigonally distorted octahedral geometry in the tris-catecholate binding mode.[54] The signals at $g \approx 4.2$ of both spectra of the heterodinuclear species exhibit more asymmetric features than those of the iron(III) mononuclear complex (see Fig. 7), which can be attributed to the presence of more than one metal centre in solution.[53,54] Indeed

Table 7 Rhombic distortion (E/D) and effective *g* values expected from the high-spin species of $Cu^{2+}/Fe^{3+}/H_6L^1$ 1 : 1 : 1 ratio solutions at pH 4.6 and 10.2. The values observed in the experimental spectra are in italics

pH	E/D	Doublet	g_1	g_2	g_3
4.6	0.126	$\|\pm 5/2>$	9.963	0.99	0.113
		$\|\pm 3/2>$	*5.534*	2.495	2.752
		$\|\pm 1/2>$	1.57	*8.395*	3.135
	0.278	$\|\pm 5/2>$	9.791	0.440	0.585
		$\|\pm 3/2>$	*4.597*	*3.955*	*4.200*
		$\|\pm 1/2>$	0.805	9.516	1.216
10.2	0.288	$\|\pm 5/2>$	9.773	0.469	0.630
		$\|\pm 3/2>$	4.539	*4.019*	*4.229*
		$\|\pm 1/2>$	0.766	*9.551*	1.141

the peak to peak line width for the signal at 1570 G is 20 G (pH 4.6) and 30 G (pH 10.2) while the value for the mononuclear complex is about 10 G (at pH 10).

The broader hyperfine structure of the spectrum at pH 10.2 in the $\Delta M_s = \pm 1$ transition with an average coupling constant of 75.16 G indicates the presence of the second metal ion. The hyperfine pattern is normally more complicated when the coupling between the two metal centres is weak.[56] The four (a–d in Fig. 9a) and five (1–5 in Fig. 9b) resonances clearly observed at $g =$ 1.849, 1.887, 1.926, 1.968 (pH 4.6) and 1.828, 1.865, 1.904, 1.944, 1.986 (pH 10.2) are associated with the presence of coupled metal centres, see Fig. 9. Therefore the EPR spectra clearly testify the formation of the copper(II)/iron(III) heterodinuclear complexes of H_6L^1 with two metal centres, which are weakly coupled.[56–58]

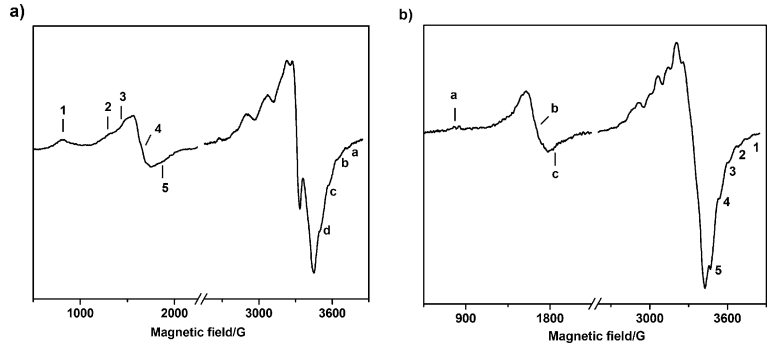

Fig. 9 EPR spectrum of the $Cu^{2+}/Fe^{3+}/H_6L^1$ 1 : 1 : 1 ratio solutions at 4.6 (a) and 10.2 (b) pH values in water–DMSO (1 : 1 v/v), recorded at 5 K. Microwave power of 2.35 mW, modulation amplitude of 1 mT and frequency of 9.64 GHz.

Conclusions

Spectroscopic and/or potentiometric studies have shown that the new ditopic macrocyclic ligand with tris-catecholate arms, H_6L^1, forms heterodinuclear Cu^{2+}/Fe^{3+} and Cu^{2+}/Zn^{2+} complexes due to the presence of two distinct and distant types of donor atom in the H_6L^1 molecule.

The acid–base behaviour of the ligand is characteristic of the two types of basic centre in the molecule, the tetraaza macrocycle and the catecholate moieties. It was shown that the H_6L^1 ligand is very selective for the Fe^{3+} ion, forming mono-and dinuclear complexes. The high stability constant of the $[FeL^1]$ complex is explained by the strong coordination of the tris-catecholate to the iron in a distorted octahedral geometry. As expected for a catecholate ligand, the mononuclear copper(II) and zinc(II) complexes are formed only at very high pH, which precluded the determination of the stability constants of these species. The H_6L^1 ligand did not show special affinity for the Zn^{2+} ion, but a much more significant one for the Cu^{2+} ion. The electronic data of Cu^{2+}/H_6L^1 solutions suggested the equilibrium between complexes with the copper coordinated to the macrocycle and in the catecholate arms. The EPR spectrum of the $[Cu_2L^1]^{2-}$ complex showed typical features for a dinuclear complex with weak interactions between the two copper(II) centres.

The study of $Cu^{2+}/Fe^{3+}/H_6L^1$ 1 : 1 : 1 ratio aqueous solutions revealed that mononuclear protonated iron(III) complexes are formed at very low pH values and then protonated heterodinuclear species are formed. At pH 7.5 the non-protonated heterodinuclear $[CuFeL^1]^-$ complex is formed in ≈ 95%. UV-vis and EPR spectroscopic studies revealed that the copper is coordinated to the amine donors of the macrocyclic moiety and the iron to the oxygen donors from the catecholate of the arms. The interaction between both paramagnetic centres is weak, as expected due to the relative length of the arms.

The heterodinuclear $[CuFeL^1]^-$ and $[CuZnL^1]^{2-}$ complexes may be explored as simple models of the active sites of cytochrome c oxidase and bovine erythrocyte superoxide dismutase and the $[Cu_2L^1]^{2-}$ complex as a model of dicopper tyrosinases.

Experimental

General

Microanalyses were carried out by the ITQB Microanalytical service, and the IR spectra were recorded from KBr pellets on a UNICAM Mattson 7000 spectrometer.

Reagents

3,4-Dimethoxybenzoyl chloride (98% purity) and boron tribromide (99% of purity) were obtained from Aldrich. All the chemicals were of reagent grade and used as supplied without further purification. 3,7,11-Tris(3-aminopropyl)-3,7,11,17-tetraazabicyclo[11.3.1]heptadeca-1(17),13,15-triene (L^{12}) was synthesized and characterized as reported.[13] The organic solvents were purified by standard methods.[59] The reference used for the ^{1}H NMR measurements in D_2O was 3-(trimethylsilyl)-propanoic acid-d_4-sodium salt and in $CDCl_3$ and Me_2SO-d_6 the solvent itself.

Syntheses

3,7,11-Tris[*N*-(3,4-dimethoxybenzoyl)-(3-aminopropyl)]-3,7,11,17-tetraazabicyclo[11.3.1]heptadeca-1(17),13,15-triene, L^{1p}. 3,4-Dimethoxybenzoyl chloride (1.54 g, 7.7 mmol) dissolved in dry CH_2Cl_2 (15 cm^3) was added dropwise to the stirred solution of L^{12} (1.04 g, 2.6 mmol) in water–CH_2Cl_2 (35 cm^3) simultaneously with 50 cm^3 of 0.1 mol dm^{-3} sodium hydroxide (50 cm^3) during about 30 min. Then the mixture was stirred for 2 h, and the layers were separated. The aqueous layer was extracted with 4 × 20 cm^3 of CH_2Cl_2. The combined CH_2Cl_2 solutions were dried over Na_2SO_4 and evaporated to dryness. Recrystallization from ethyl acetate–cyclohexane afforded white-yellow flakes of the methyl catecholate protected L^{1p}. Yield: 85%. R_f (10% CH_3OH–CH_2Cl_2) 0.37. ^{1}H NMR (300 MHz, $CDCl_3$) δ 1.503 (q, 4 H, $N^{3,11}CH_2CH_2CH_2N^7$), 1.583 (q, 2 H, $N^7CH_2CH_2CH_2NH$), 1.795 (q, 4 H, $N^{3,11}CH_2CH_2CH_2NH$), 2.385 (br, 6 H, $N^{3,11}CH_2CH_2$, $N^7CH_2CH_2$), 2.486 (t, 4 H, J = 6 Hz, $N^{3,11}CH_2CH_2$), 2.624 (t, 4 H, J = 6 Hz, $N^7CH_2CH_2$), 3.230 (t, 2 H J = 5.4 Hz, CH_2CH_2NH), 3.522 (t, 4 H, J = 5.7 Hz, CH_2CH_2NH), 3.567 (s, 4 H, $N^{3,11}CH_2CH$), 3.779, 3.836 and 3.856 [s, 3 × 6 H, OCH_3], 6.712 (d, 2 H, J = 8.4 Hz, CH^{bz}), 6.766 (d, 1 H, J = 8.4 Hz, CH^{bz}), 7.077 (d, 2 H, J = 7.5 Hz, CH^{py}), 7.171 (d, 2 H, J = 1.8 Hz, CH^{bz}), 7.353 (d, 1 H, J = 1.8 Hz, CH^{bz}), 7.383 (d, 2 H, J = 1.8 Hz, CH^{bz}), 7.435 (d, 1 H, J = 2.1 Hz, CH^{bz}), 7.704 (t, 1 H, CH^{py}). ^{13}C NMR (300 MHz, $CDCl_3$) δ 24.03 ($N^7CH_2CH_2CH_2N^{3,11}$) 25.83, 26.67, 38.74, 39.26, 51.97, 52.09, 52.55, 54.20, 56.12 and 56.19 (OCH_3), 60.18 ($N^{7,11}CH_2CH$), 110.3, 110.4, 110.9, 111.0 and 119.8 (CH^{bz}), 119.9 (CH^{py}), 122.8 (CH^{bz}), 127.4 and 127.7 (C^{bz}), 137.1 (CH^{py}), 148.9, 149.0, 151.6 and 151.7 (C^{bz}), 158.4 (C^{py}) 167.2 and 167.59 (C=O). IR (KBr, cm^{-1}): 3429, 2962, 2929, 2838 (OCH_3), 1705 and 1636 (C=O), 1604 (C–C ring), 1583, 1550 and 1509 (N–H), 1463 (C^{bz}–C=O), 1441, 1383, 1339, 1262, 1229, 1180, 1129, 1101, 1021, 874, 800, 764, 668 and 631. Found: C, 63.22; N, 10.53; H, 8.08. Calc. for $C_{49}H_{67}N_7O_9 \cdot 2H_2O$: C, 63.02; N, 10.53; H, 7.60%.

3,7,11-Tris[*N*-(3,4-dihydroxybenzoyl)-(3-aminopropyl)]-3,7,11,17-tetraazabicyclo[11.3.1]heptadeca-1(17),13,15-triene, H_6L^1. BBr_3 (3.5 cm^3, 29 mmol) was added dropwise through a syringe to a stirring solution of L^{1p} (0.155 g, 0.23 mmol) in dry CH_2Cl_2 (4 cm^3), at 0 °C and under N_2. The resulting white-yellow suspension was allowed to stir during 2 d at r.t. Then to the reaction mixture, CH_3OH (10 cm^3) was added at 0 °C and the clear solution was stirred at r.t during 4 h. Upon repeated addition and evaporation of CH_3OH (10 × 10 cm^3) to remove the borate ester, the product was dissolved in CH_3OH, precipitated with Et_2O and collected by filtration. The final product, which is a light beige, crystalline and very hygroscopic powder, was dried under vacuum. Yield: 56%. ^{1}H NMR (300 MHz, DMSO-d_6) δ: 1.648 (br, 2 H, $N^7CH_2CH_2CH_2NH$), 1.920 (br, 8 H, CH_2), 2.724 (br, 2 H, CH_2), 2.888 (br, 6 H, CH_2), 3.022 (br, 10 H, CH_2), 3.369 (br, 2 H), 4.294 (s, 4 H, $N^{3,11}CH_2CH$), 6.762 (d, 3 H, J = 8.1 Hz, CH^{bz}), 7.171 (d, 3 H, J = 7.8 Hz, CH^{bz}), 7.246 (d, 3 H, CH^{bz}), 7.486 (d, 2 H, J = 7.8 Hz, CH^{py}), 7.841, (t, 1 H, J = 8.1 Hz, CH^{py}), 8.201, (t, 1 H, J = 5.4 Hz, NH), 8.266, (t, 2 H, J = 6.9 Hz, NH), 9.082 and 9.507 (s, OH). ^{13}C NMR (300 MHz, D_2O) δ 21.93, 26.82, 29.71, 37.68, 38.48, 50.74, 51.28, 51.64, 53.62, 59.65, 110.1, 110.3, 110.8, 112.5, (CH^{bz}), 119.9, (CH^{py}), 120.2 and 122.9, (CH^{bz}), 123.3 and 127.3, (C^{bz}), 137.1 (CH^{py}), 148.3 and 148.8

(C^{bz}), 151.6, 151.8 (C^{bz}), and 157.9 (C^{py}), 167.4 and 171.7 (C=O). IR (KBr, cm^{-1}): 3378 (OH), 1633 (C=O), 1597, 1538, 1515 (N–H), 1457 (C^{bz}–C=O), 1440, 1384, 1314, 1290, 1251, 1198, 1141, 1112, 1060, 952, 877, 826, 784, 760, 633. Found: C, 44.76; N, 8.37; H, 4.89. Calc. for $C_{43}H_{59}Br_4N_7O_9.H_2O$: C, 44.70; N, 8.40; H, 4.95%.

Potentiometric measurements

Reagents and solutions. Metal ion solutions were prepared at 0.025–0.050 mol dm^{-3} from the nitrate salts of the metals of analytical grade with demineralized water (from a Millipore/Milli-Q system). The solutions were standardized by titration with Na_2H_2edta.[60] The carbonate free solution of the titrant, KOH, was prepared and discarded as described previously.[13,28] For the back titrations a 0.100 mol dm^{-3} solution of HNO_3 was used.

Equipment and work conditions. The equipment used was described previously.[13,28] The temperature was kept at 298.2 ± 0.2 K and atmospheric CO_2 was excluded from the cell during the titration by passing purified nitrogen across the top of the experimental solution in the reaction cell. The ionic strength of the solutions was kept at 0.10 mol dm^{-3} with KNO_3.

Measurements. The [H$^+$] of the solutions was determined by the measurement of the electromotive force of the cell, $E = E'^{\circ} + Q \log [H^+] + E_j$, E'°, Q, E_j and $K_w = ([H^+][OH^-])$ were obtained as described previously.[13,28] The value of K_w was found to be equal to $10^{-13.80}$ mol^2 dm^{-6}.

Potentiometric equilibrium measurements were carried out using 15.00 or 20.00 cm^3 of ≅ 2.00–3.00 × 10^{-3} mol dm^{-3} ligand solution diluted to a final volume of 25.00 or 30.00 cm^3, in the absence of metal ions, in the presence of each metal ion or in which the $C_M : C_L$ ratios were 1 : 1 and 2 : 1, or in the presence of two metal ions for which the $C_M : C_{M'} : C_L$ ratios were 1 : 1 : 1 and 1 : 1 : 2. A minimum of two replicate measurements was taken.

The equilibrium for the formation of complexes with two metal ions and H_6L^1 was very slow to attain. Back titrations with standard HNO_3 solutions were performed to confirm the values of the final E readings.

Calculation of equilibrium constants

Protonation constants $K^{S}{}_{O}{}^{Hs} = [H_iL]/[H_{i-1}L] \times [H^+]$ (i = 1–6) were calculated by fitting the potentiometric data obtained for the free ligand, using the HYPERQUAD program.[61] Stability constants of the various species formed in solution were obtained from the experimental data corresponding to the potentiometric titration of solutions of the different metal ions each of them with different metal to ligand ratios also using the HYPERQUAD program. The initial computations were obtained in the form of overall stability constants, $\beta_{M_mH_hL_l} = [M_mH_hL_l]/([M]^m \times [H^+]^h \times [L]^l$. Mononuclear species, $M(H_iL^1)$, (i = 0–7), and homodinuclear species $M_2(H_iL^1)$ (i = 0–2) and $M_2H_{-i}L$ (i = 1–3) were formed [$\beta_{(M2(H-1)iL} = \beta_{(M2L(OH)i} \times (K_w)^i$. The overall stability constants for the heterodinuclear species are defined as $\beta_{M_mM_{m'}H_hL_l} = [M_mM_{m'}H_hL_l]/([M]^m \times [M']^{m'} \times [H^+]^h \times [L]^l$. Differences, in log units, between the values of protonated or hydrolysed and non-protonated constants, respectively for the mono- and dinuclear species, provide the stepwise reaction constants. The species considered in a particular model were those that could be justified by the principles of coordination chemistry. The errors quoted in Tables 2 and 5 are the standard deviations of the overall stability constants given directly by the program for the input data, which include all the experimental points of all the titration curves.

Spectroscopic studies

All the NMR measurements were performed on a Bruker CXP-300 or a Bruker DRX-500 spectrometer. Electronic spectra were recorded on a UNICAM model UV-4 or a Shimadzu model UV-3100 spectrometer. Aqueous solutions of 2 × 10^{-4}–2.0 × 10^{-5} mol dm^{-3} were used to record spectra in the UV region and ≃ 1.0 × 10^{-3} mol dm^{-3} in the other regions. EPR spectroscopic measurements were recorded with a Bruker ESP 380 spectrometer equipped with continuous-flow cryostats for liquid helium or liquid nitrogen, operating at X-band. The complexes were prepared at 4.0 × 10^{-3}–1 × 10^{-2} mol dm^{-3} in aqueous or DMSO–H_2O (1 : 1 v/v) solutions. The spectra of all complexes were recorded at 5 to 13 K.

Acknowledgements

The authors acknowledge H. Pereira-Matias for help with the 2D NMR experiments, M. Pereira for the acquisition of EPR spectra, and M. C. Almeida for the elemental analysis data. K. P. Guerra also acknowledges FCT for a grant (SFRH/BD/6492/2001).

References

1 A. L. Gavrilova and B. Bosnich, *Chem. Rev.*, 2004, **104**, 349.
2 M. M. Pereira, M. Santana and M. Teixeira, *Biochim. Biophys. Acta*, 2001, **1505**, 185.
3 A. Decker and E. I. Solomon, *Curr. Opin. Chem. Biol.*, 2005, **9**, 152.
4 I. A. Koval, P. Gamez, C. Belle, K. Selmeczi and J. Reedijk, *Chem. Soc. Rev.*, 2006, **35**, 814.
5 E. Kim, M. E. Helton, S. Lu, P. M. Loccoz, C. D. Incarvito, A. L. Rheingold, S. Kaderli, A. D. Zuberbühler and K. D. Karlin, *Inorg. Chem.*, 2005, **44**, 7014.
6 L. Que, Jr. and W. B. Tolman, *Angew. Chem., Int. Ed.*, 2002, **41**, 1114.
7 R. F. Pasternack, E. J. Gibbs and J. J. Villafranca, *Biochemistry*, 1983, **22**, 2406.
8 A. E. V. Gorden, J. Xu, K. N. Raymond and P. Durbin, *Chem. Rev.*, 2003, **103**, 4207.
9 J. Costamagna, G. Ferraudi, B. Matsuhiro, M. Campos-Vallette, J. Canales, M. Villagrán, J. Vargas and M. J. Aguirre, *Coord. Chem. Rev.*, 2000, **196**, 125.
10 P. Guerriero, S. Tamburini and P. A. Vigato, *Coord. Chem. Rev.*, 1995, **139**, 17.
11 F. L. Weitl and K. N. Raymond, *J. Am. Chem. Soc.*, 1979, **101**, 2728.
12 S. J. Rodgers, C.-W. Lee, C. Y. Ng and K. N. Raymond, *Inorg. Chem.*, 1987, **26**, 1622.
13 K. P. Guerra, R. Delgado, M. G. B. Drew and V. Félix, *Dalton Trans.*, 2006, 4124.
14 L. D. Loomis and K. N. Raymond, *Inorg. Chem.*, 1991, **30**, 906.
15 W. R. Harris and K. N. Raymond, *J. Am. Chem. Soc.*, 1979, **101**, 6534.
16 L. Alderighi, P. Gans, A. Ienco, D. Peters, A. Sabatini and A. Vacca, *Coord. Chem. Rev.*, 1999, **184**, 311.
17 L. D. Pettit and H. K. J. Powell, *IUPAC Stability Constants Database*, Academic Software, Timble, 2003.
18 A. Avdeef, S. R. Sofen, T. L. Bragante and K. N. Raymond, *J. Am. Chem. Soc.*, 1978, **100**, 5362.
19 W. R. Harris, K. N. Raymond and F. L. Weitl, *J. Am. Chem. Soc.*, 1981, **103**, 2667.
20 Z. Hou, T. D. P. Stack, C. J. Sunderland and K. N. Raymond, *Inorg. Chim. Acta*, 1997, **263**, 341.
21 B. P. Hay, D. A. Dixon, R. Vargas, J. Garza and K. N. Raymond, *Inorg. Chem.*, 2001, **40**, 3922.
22 D. Imbert, F. Thomas, P. Baret, G. Serratrice, D. Gaude, J.-L. Pierre and J.-P. Laulhère, *New J. Chem.*, 2000, **24**, 281.

23 J. Costa and R. Delgado, *Inorg. Chem.*, 1993, **32**, 5257.
24 J. R. Telford and K. N. Raymond, *Inorg. Chem.*, 1998, **37**, 4578.
25 W. R. Harris, C. J. Carrano, S. R. Cooper, S. R. Sofen, A. E. Avdeef, J. V. McArdle and K. N. Raymond, *J. Am. Chem. Soc.*, 1979, **101**, 6097.
26 M. E. Cass, T. M. Garrett and K. N. Raymond, *J. Am. Chem. Soc.*, 1989, **111**, 1677.
27 V. L. Percoraro, F. L. Weitl and K. N. Raymond, *J. Am. Chem. Soc.*, 1981, **103**, 5133.
28 K. P. Guerra, R. Delgado, L. M. P. Lima, M. G. B. Drew and V. Félix, *Dalton Trans.*, 2004, 1812.
29 M. J. Kappel and K. N. Raymond, *Inorg. Chem.*, 1982, **21**, 3437.
30 J. Costa, R. Delgado, M. G. B. Drew and V. Félix, *J. Chem. Soc., Dalton Trans.*, 1998, 1063.
31 F. Biaso, P. Baret, J.-L. Pierre and G. Serratrice, *J. Inorg. Biochem.*, 2002, **89**, 123.
32 T. H. Stevens, G. W. Brudvig, D. F. Bocian and S. I. Chan, *Proc. Natl. Acad. Sci. USA*, 1979, **76**, 3320.
33 J. A. Tainer, E. D. Getzoff, J. S. Richardson and D. C. Richardson, *Nature*, 1983, **306**, 284.
34 T. Plenge, R. Dillinger, L. Santagostini, L. Casella and F. Tuczek, *Z. Anorg. Allg. Chem.*, 2003, **629**, 2258.
35 L. Casella, E. Monzani, M. Gullotti, D. Cavagnino, G. Cerina, L. Santagostini and R. Ugo, *Inorg. Chem.*, 1996, **35**, 7516.
36 F. Neese, Diploma Thesis, University of Konstanz, Germany, 1993.
37 J. Costa, R. Delgado, M. G. B. Drew, V. Félix and A. Saint-Maurice, *J. Chem. Soc., Dalton Trans.*, 2000, 1907.
38 J. Costa, R. Delgado, M. C. Figueira, R. T. Henriques and M. Teixeira, *J. Chem. Soc., Dalton Trans.*, 1996, 65.
39 B. J. Hathaway, *Coord. Chem. Rev.*, 1983, **52**, 87.
40 V. Félix, M. J. Calhorda, J. Costa, R. Delgado, C. Brito, M. T. Duarte, T. Arcos and M. G. B. Drew, *J. Chem. Soc., Dalton Trans.*, 1996, 4543.
41 U. Sakaguchi and A. W. Addison, *J. Chem. Soc., Dalton Trans.*, 1979, 600.
42 E. F. Hasty, L. J. Wilson and D. N. Hendrickson, *Inorg. Chem.*, 1978, **17**, 1834.
43 D. E. Wilcox, J. R. Long and E. I. Solomon, *J. Am. Chem. Soc.*, 1984, **106**, 2186.
44 A. Riesen, M. Zehnder and T. A. Kaden, *Helv. Chim. Acta*, 1986, **69**, 2074.
45 E. I. Solomon, U. M. Sundaram and T. E. Machonkin, *Chem. Rev.*, 1996, **96**, 2563.
46 T. R. Felthouse and D. N. Hendrickson, *Inorg. Chem.*, 1978, **17**, 444.
47 S. S. Tandon, L. K. Thompson, J. N. Bridson and J. C. Dewan, *Inorg. Chem.*, 1994, **33**, 54.
48 S. El Ghachtouli, C. Cadiou, I. D. Olivier, F. Chuburu, M. Aplincourt, V. Turcry, M. Le Baccon and H. Handel, *Eur. J. Inorg. Chem.*, 2005, 2658.
49 E. Monzani, L. Quinti, A. Perotti, L. Casella, M. Gullotti, L. Randaccio, S. Geremia, G. Nardin, P. Faleschini and G. Tabbì, *Inorg. Chem.*, 1998, **37**, 553.
50 S. S. Eaton and G. R. Eaton, *J. Am. Chem. Soc.*, 1982, **104**, 5002.
51 T. B. Kaprishin, M. S. Gebhard, E. I. Solomon and K. N. Raymond, *J. Am. Chem. Soc.*, 1991, **113**, 2977.
52 G. P. Horsman, A. Jirasek, F. H. Vaillancourt, C. J. Barbosa, A. A. Jarzecki, C. Xu, Y. Mekmouche, T. G. Spiro, J. D. Lipscomb, M. W. Blades, R. F. B. Turner and L. D. Eltis, *J. Am. Chem. Soc.*, 2005, **127**, 16882.
53 V. L. Pecoraro, G. B. Wong, T. A. Kent and K. N. Raymond, *J. Am. Chem. Soc.*, 1983, **105**, 4617.
54 J. T. Weisser, M. J. Nilges, M. J. Sever and J. J. Wilker, *Inorg. Chem.*, 2006, **45**, 7736.
55 W. R. Hagen, *Adv. Inorg. Chem.*, 1992, **38**, 165.
56 A. Bencini and D. Gatteschi, *EPR of Exchange Coupled Systems*, Springer-Verlag, Berlin, 1990.
57 M. R. Cheesman, V. S. Oganesyan, N. J. Watmough, C. S. Butler and A. Thomson, *J. Am. Chem. Soc.*, 2004, **126**, 4157.
58 M. J. Gunter, L. N. Mander, K. S. Murray and P. E. Clark, *J. Am. Chem. Soc.*, 1981, **103**, 6784.
59 D. D. Perrin and W. L. F. Armarego, *Purification of Laboratory Chemicals*, Pergamon, Oxford, 3rd edn, 1988.
60 G. Schwarzenbach and W. Flaschka, *Complexometric Titrations*, Methuen & Co, London, 1969.
61 P. Gans, A. Sabatini and A. Vacca, *Talanta*, 1996, **43**, 1739.

